Inorganic Chemistry

ARTICLE

pubs.acs.org/IC

Luminescent Copper(I) Halide Adducts of $[Au(im(CH_2py)_2)_2]PF_6$ Exhibiting Short Au(I)···Cu(I) Separations and Unusual Semibridging NHC Ligands

Christoph E. Strasser and Vincent J. Catalano*

Department of Chemistry, University of Nevada, Reno, Nevada 89557, United States

Supporting Information

ABSTRACT: The picolyl-substituted NHC complex $[Au(im(CH_2py)_2)_2]PF_6$ (**1**) reacts with two equivalents of copper(I) halides, affording compounds $[Au(im(CH_2py)_2)_2(CuX)_2]PF_6$ (X = Cl, **2**; Br, **3**; I, **4**). Each complex contains a nearly linearly coordinated $[Au(NHC)_2]^+$ center where the two picolyl groups on each $im(CH_2py)_2$ ligand chelate a single copper atom. The Cu(I) center resides in a distorted tetrahedral environment and is coordinated to two pyridyl groups, a halide ion, and a gold metalloligand. The Au(I)−Cu(I) separations measure 2.7030(5), 2.6688(9), and 2.6786(10) Å for **2**−**4**, respectively. Additionally, each Cu(I) center is further coordinated by a semibridging NHC ligand with short Cu−C separations of ∼2.3 Å. In solution, these complexes dissociate the Cu(I) ion. In the solid state, **2**−**4** are photoluminescent with respective emission maxima of 512, 502, and 507 nm. The reaction of $[Au(im(CH_2py)_2)_2]PF_6$ with four equivalents of CuBr afforded the coordination polymer $\{[AuCu_2Br_2(im(CH_2py)_2)_2]Br\cdot 3CH_3CN\}_n$ (**5**). This polymeric complex contains $[Au(NHC)_2]^+$ units interconnected by Cu_2Br_2 dimers. In **5**, the Au−Cu separations are long at 4.23 and 4.79 Å, while the Cu−Cu distance is considerably shorter at 2.9248(14) Å. In the solid state, **5** is photoluminescent with a broad band appearing at 533 nm.

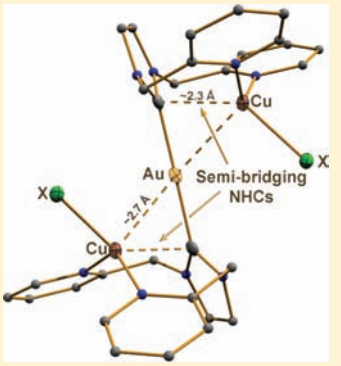

INTRODUCTION

N-heterocyclic carbenes are important ligands in organometallic chemistry.[1,2] Gold(I) NHC complexes have been extensively studied[3] and have found numerous applications in catalysis,[4−6] as have their Cu(I) and Ag(I) analogs.[5,7−10] Metallophilic interactions between the different coinage metals, i.e., metal−metal separations shorter than the sum of the van der Waals radii, have attracted considerable interest in part because these interactions often lead to interesting structural properties.[11−14] NHCs are excellent σ donors rivaling most phosphines[15] and are capable of supporting extended d^{10}−d^{10} interactions between coinage metals.[16−23] Alteration of the pendant arms produces a simple mechanism to arrange metal atoms in close proximity to each other. Such interactions frequently are the origin of luminescence processes[24] and have been utilized in the design of luminescent vapochromic sensors.[17,25,26] Previously, our group reported picolyl- and quinolyl-substituted $Au(NHC)_2^+$-type complexes acting as metalloligands toward butterfly-type Cu_2X_2 (X = Cl, Br, I) dimers with exceptionally close Au···$Cu_{2(centroid)}$ separations of ∼2.56 Å (Scheme 1).[27] Gold(I) has been shown to be a viable metalloligand that can act as a nonclassical ligand toward a variety of coordinatively unsaturated transition metal centers. Compounds having interactions between Au and Ag,[28,29] Tl,[30] Bi,[31] Cu,[29,32] Rh,[32] Ir,[32] and Mo[33] have been reported. Many of these utilize the attractive interactions between anionic bis(halophenyl)aurates and the cationic metal ion,[29−31] but neutral and even cationic gold carbene[28] and phosphine complexes[32] as well as unligated gold atoms[33] are known to associate under suitable conditions.

Scheme 1. A Butterfly-Type Cu_2Br_2 Cluster Supported by a Au···$Cu_{2(centroid)}$ Interaction[27]

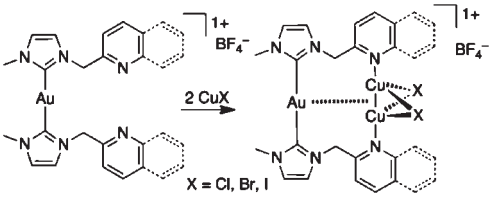

We questioned whether the Au(I) center could act as a metalloligand simultaneously to two cuprous dimers, or whether this metallo-interaction is limited to a single three-metal system. Replacing the dissymmetric methylpicolyl substituted NHC ligand (Scheme 1) with the dipicolyl-substituted NHC provides a suitable coordination environment to bind metal clusters on each side of the gold center. However, as described below, we instead discovered a new coordination motif that gave rise to bent Cu···Au···Cu chains.

RESULTS

Attempts to produce the butterfly Cu_2X_2 dimers with the symmetrical starting complex **1** analogous to those reported earlier were unsuccessful. Rather, the addition of excess cuprous

Received: August 17, 2011
Published: October 06, 2011

Scheme 2. Preparation of Complexes 2−5

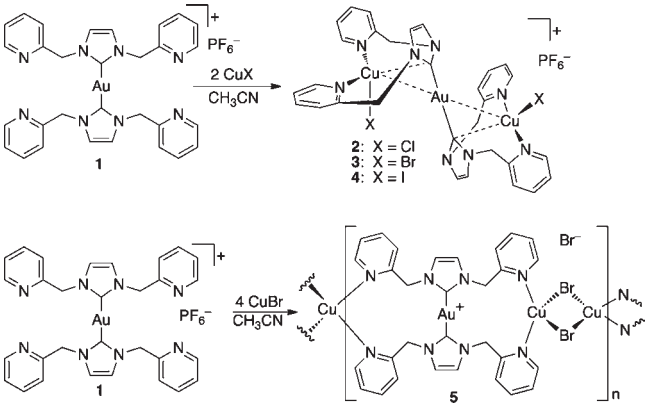

halide to **1** only produced intractable mixtures which have eluded characterization. As shown in Scheme 2, the addition of two equivalents of CuX to **1** in acetonitrile followed by crystallization with diethyl ether produces the trimetallic species $[Au(im(CH_2py)_2)_2(CuX)_2]PF_6$ (X = Cl, **2**; Br, **3**; I, **4**) in good yield. The polymeric complex **5**, which has a similar formulation to that of **3**, was isolated after the addition of four equivalents of CuBr to warm solutions of **1** followed by slow cooling. Here, each Au(I) complex is interconnected by a Cu_2Br_2 unit to form an extended linear polymer with a bromide ion balancing the overall monocationic charge. Analogous reactions with four equivalents of CuCl or CuI led to mixtures of complexes that did not yield X-ray-quality crystals.

In acetonitrile-d_3 solution, the ^1H NMR spectra for **2**−**4** are nearly identical to that of **1**, with singlets for the imidazole backbone and methylene protons indicating that the CuX dissociates in solution. The ^{13}C carbene resonance of **2** appears at 171.6 ppm in the solid-state CP-MAS spectrum (see the Supporting Information, Figure S15), which also shows two sets of signals for C-2, C-4, and C-6 in the pyridine rings, as is expected for a crystallographically unique ligand (see below). The resonances for C-3, C-5, and the imidazole backbone carbon atoms appear between 125 and 123 ppm. In **3** (Figure S16, Supporting Information), the carbene resonance appears at 171.2 ppm. The positions of the signals for the pyridine rings are essentially unchanged when CuX is coordinated to **1**; no trend within the halide series is evident. Additional signals corresponding to C-2 and C-4 pyridine are observed in the spectra of **2** and **3** relative to that of **1**, indicating a less symmetrical environment around the two picolyl pendant arms. The more symmetrical environment of the polymeric system, **5**, is manifested in the solid-state ^{13}C CP-MAS NMR spectrum, where the four picolyl groups reside in magnetically similar environments. The respective signals for C-2 and C-6 only give rise to broad unresolved signals, while two environments for C-4 are evident (Figure S17, Supporting Information). Additionally, the carbene resonance of **5**, which appears at 185.5 ppm, is relatively unperturbed by the Cu_2Br_2 unit. In the unsubstituted starting material **1**, the carbene carbon resonates at 187.2 ppm.

In the gas phase, compounds **2**−**4** appear to stay intact. Peaks with the proper isotopomer ratios corresponding to the preformed cations $[Au(im(CH_2py)_2)_2(CuX)_2]^+$ were observed in electrospray high-resolution mass spectrometry (see the Supporting Information, Figures S4−S6). Fragmentation occurs via the loss of one ligand and copper(I) halide, forming the bimetallic $[AuCuX(im(CH_2py)_2)]^+$ species, or by the complete loss of both CuX units, producing $[Au(im(CH_2py)_2)_2]^+$ (**1**). The polymeric complex **5** yields several clusters incorporating one or two ligands, one gold atom, and varying numbers of Cu^+ and Br^- ions, along with the gold-free $[Cu_2Br(im(CH_2py)_2)]^+$.

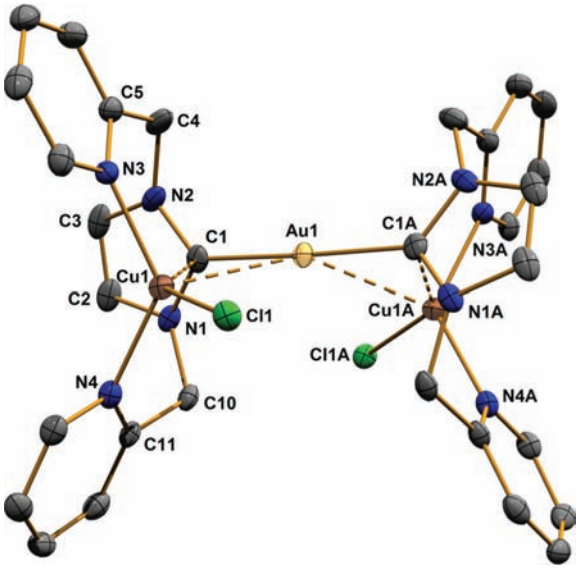

Figure 1. Structure of the cationic portion of **2** drawn with 50% probability ellipsoids. Hydrogen atoms are omitted for clarity. Atoms labeled with A are related by a 2-fold rotation.

Table 1. Bond Lengths (Å) and Angles (deg) for Compounds 2−4[a]

	2 (X = Cl)	**3** (X = Br)	**4** (X = I)
Au1···Cu1	2.7030(5)	2.6688(9)	2.6786(10)
Au1−C1	2.046(4)	2.049(6)	2.054(9)
Cu1−C1	2.310(3)	2.303(7)	2.271(8)
Cu1−X1	2.3138(10)	2.4359(10)	2.5476(12)
Cu1−N3	2.049(3)	2.043(5)	2.046(7)
Cu1−N4	2.036(3)	2.024(5)	2.029(8)
Cu1−Au1−Cu1A	148.56(2)	160.82(4)	163.07(5)
C1−Au1−C1A	177.9(2)	175.9(4)	174.7(5)
N3−Cu1−N4	129.13(13)	130.1(2)	130.2(3)
Au1−Cu1−X1	91.74(3)	89.38(3)	88.03(4)
C1−Cu1−X1	138.89(10)	136.86(17)	135.5(2)
N2−C4−C5	113.2(3)	113.0(5)	113.4(7)
N1−C10−C11	109.8(3)	110.7(6)	110.9(7)

[a] Symmetry operators: (A): $-x + 1, y, -z + 1/2$.

Compounds **2**−**5** were further characterized by single-crystal X-ray diffraction (see Figure 1 for the structure of the cationic portion of **2**). Selected bond lengths and angles are presented in Tables 1 and 2, while crystallographic parameters are listed in Table 3. Even though compounds **2**−**4** are isomorphous and crystallize in the monoclinic space group $C2/c$, there are notable differences in their solid state structures. The ease of crystallization under comparable conditions follows the order **2** ≥ **3** ≫ **4**, the latter crystallizing very slowly and therefore affording a very

dx.doi.org/10.1021/ic201795b |*Inorg. Chem.* 2011, 50, 11228–11234

low yield of crystalline product. As shown in Figures 2−4, each crystal structure contains one-half of the cation in the asymmetric unit, with the remaining generating a 2-fold rotation axis through the gold center. Each cation contains a nearly linearly coordinated Au(I) center coordinated to two NHC moieties where both picolyl groups on each $im(CH_2py)_2$ ligand bridge a single copper atom. The metal atoms form a bent chain with short Au1−Cu1 separations of 2.7031(5) Å for **2**, 2.6688(9) Å for **3**, and 2.6786(10) Å for **4**. The intermetallic Cu1−Au1−Cu1A angles for **3** and **4** are close at 160.82(4) and 163.07(5)°; however, this angle is contracted to only 148.56(2)° in the chloro-containing species (**4**). The coordination environment around the copper center is quite distorted. In addition to the coordination to two pyridyl groups, a halide, and the gold metalloligand, each Cu(I) center maintains a short contact of ∼2.3 Å to the carbene carbon atom on the NHC ligand. The shortest Cu1−C1 separation of 2.271(8) Å is found in the iodo species (**4**), while the longest separation at 2.310(3) Å is measured in the chloro species (**2**). This trend is reversed in the Au1−C1 separations that lengthen as the Cu1−C1 separations shorten. For example, a Au1−C1 separation of 2.054(9) Å is measured in **4**, while in **2**, this shortens to 2.046(4) Å.

The nearly colorless polymeric compound **5**·$3CH_3CN$ crystallizes in the monoclinic spacegroup $P2/n$ upon slow cooling of an acetonitrile solution from 55 °C to room temperature. As shown in Figure 4, this compound does not incorporate PF_6^- anions from the starting material. Rather, a $CuBr_2^-$ unit interconnects two cationic $[Au(NHC)_2]^+$ units to form the extended linear polymeric array, and a lone bromide ion balances the overall charge. The Au(I) center is nearly linearly coordinated to two NHC ligands, which are related by a crystallographic 2-fold axis. Unlike the previous complexes, the Cu(I) center in **5** coordinates to two pyridyl groups on opposing ligands and completes its distorted tetrahedral environment through coordination to two bridging bromide ions. Selected bond distances

Table 2. Selected Bond Distances (Å) and Angles (deg) for 5·3CH$_3$CN[a]

	3·CH$_3$CN
Au1···Cu1	4.230
Au1···Cu2	4.789
Cu1−Cu2	2.9248(14)
Au1−C1	2.000(5)
Cu1−Br1D	2.5266 (7)
Cu2−Br1	2.5851 (8)
Cu1−N3	2.010(5)
Cu2−N4	2.049(5)
C1−Au1−C1A	175.9(3)
N3−Cu1−N3A	127.8 (3)
N4−Cu2−N4A	136.6 (3)
N3−Cu1−Br1	104.07(13)
Br1−Cu2−Br1A	112.09(4)
Br1D−Cu1−Br1E	108.32(4)
N3−Cu1−Br1D	98.46(13)
N3−Cu1−Br1E	106.60(13)
N4−Cu2−Br1	104.07(13)
N4−Cu2−Br1A	104.37(13)
Cu1B−Br1−Cu2	69.79(3)

[a] Symmetry codes: (A) $-x+3/2, y, -z+1/2$; (B) $x, y-1, z$; (C) $-x+1/2, y-1, -z+1/2$; (D) $x, y+1, z$; (E) $-x+3/2, y+1, -z+1/2$.

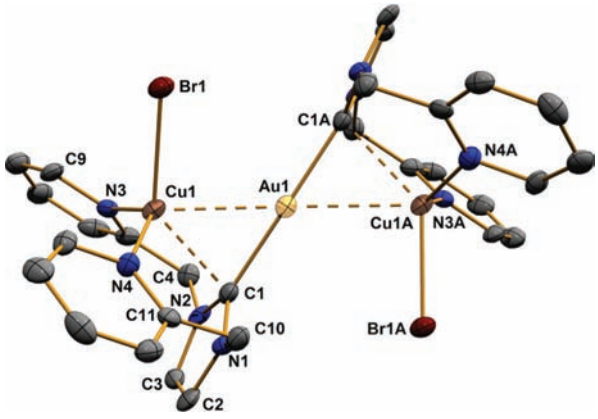

Figure 2. Thermal ellipsoid plot (50%) of **3** viewed along the C_2 axis through Au1. Hydrogen atoms and the PF_6^- anion are not shown for clarity. Atoms labeled with A are related by a 2-fold rotation.

Table 3. Crystallographic Data and Parameters for the Crystal Structures

compound	2	3	4	5·3CH$_3$CN
formula	$C_{30}H_{28}AuCl_2Cu_2F_6N_8P$	$C_{30}H_{28}AuBr_2Cu_2F_6N_8P$	$C_{30}H_{28}AuCu_2F_6I_2N_8P$	$(C_{30}H_{28}AuBr_2Cu_2N_8)_nBr_n \cdot 3nCH_3CN$
fw	1040.5	1129.4	1223.4	1187.5
cryst size, mm	0.14 × 0.02 × 0.02	0.11 × 0.03 × 0.03	0.10 × 0.04 × 0.03	0.12 × 0.08 × 0.06
cryst syst	monoclinic	monoclinic	monoclinic	monoclinic
space group	$C2/c$	$C2/c$	$C2/c$	$P2/n$
a, Å	22.5248(4)	22.6371(9)	22.8467(11)	7.4834(2)
b, Å	11.5877(2)	11.7125(4)	11.8198(5)	11.9438(2)
c, Å	14.1166(2)	13.7305(5)	13.8637(6)	23.3998(5)
β, deg	117.648(1)	114.510(2)	114.175(1)	92.978(1)
V, Å^3	3263.86(9)	3312.4(2)	3415.5(3)	2088.66(8)
Z	4	4	4	2
ρ, Mg m^{-3}	2.118	2.265	2.379	1.912
μ, mm^{-1}	6.061	8.223	7.444	7.424
R_1 [$I > 2\sigma(I)$]	0.0349	0.0397	0.0469	0.0367
wR_2 (all data)	0.0500	0.0900	0.1288	0.0922

dx.doi.org/10.1021/ic201795b |*Inorg. Chem.* 2011, 50, 11228–11234

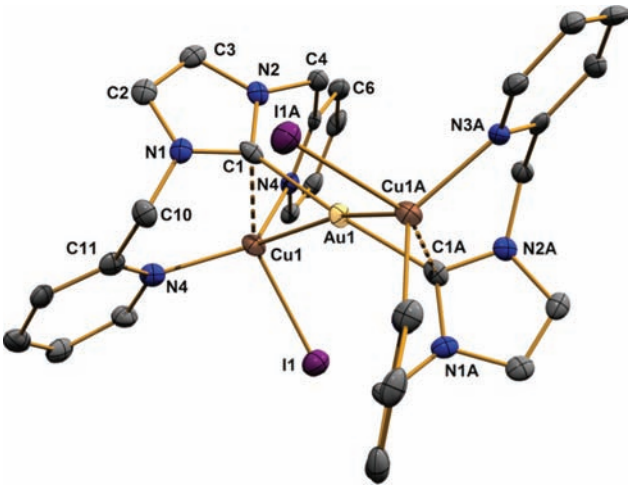

Figure 3. X-ray structural drawing with 50% thermal ellipsoids of the cationic portion of **4**. Hydrogen atoms are removed for clarity. Atoms labeled with A are related by a crystallographic 2-fold rotation.

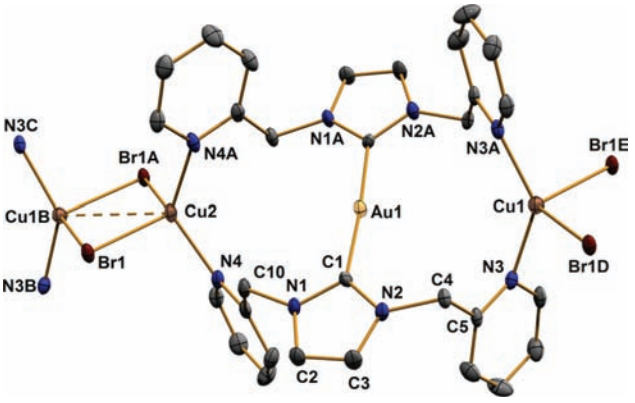

Figure 4. Molecular structure of compound $5 \cdot 3CH_3CN$ with ellipsoids drawn at the 50% probability level. The Br^- anion and acetonitrile solvents are not shown for clarity.

and angles are presented in Table 2. The lack of semibridging character in **5** relative to **2**−**4** shortens the Au1−C1 separation to 2.000(5) Å. The Au1−Cu1 and Au1−Cu2 separations are long at 4.230 and 4.789 Å; however, the Cu1−Cu2 distance is considerably shorter at 2.9248(14) Å. The angles around each copper center vary considerably with expanded N3−Cu1−N3A and N4−Cu2−N4A angles of 136.3(3) and 127.8(3)°, respectively. Br1D−Cu1−Br1E and Br1−Cu2−Br1A are more acute at 108.32(4) and 112.09(4)°. The bridging bromides span the copper dimers with Cu1−Br1−Cu2 angles of 69.79(3)° and separations of 2.5266(7) and 2.5851(8) Å for Cu1−Br1D and Cu2−Br1, respectively.

In acetonitrile solution, **2**−**5** dissociate copper, and the electronic absorption spectra are nearly identical to that of **1**. However, in the solid state at 25 °C, compounds **2**−**5** are luminescent and exhibit bright green photoemissions (Figure 5). The emission maxima do not trend according to halide. The highest energy emission band is found in the bromo-containing species, **3** (λ_{max} = 502 nm), followed closely by the iodo species, **4**, which emits at 507 nm. The chloro species, **2**, is slightly red-shifted to 512 nm. This ordering does, however, follow the trend in Au−Cu separations

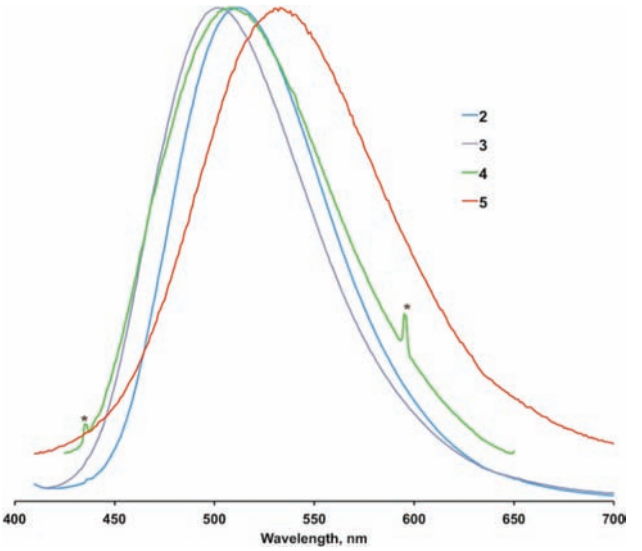

Figure 5. Normalized solid-state emission spectra of compounds **2**−**5**. The asterisks denote experimental artifacts.

with the shortest separation corresponding to the highest energy emission (complex **3**) and the lowest energy emission associated with shortest Au−Cu separation (complex **2**). The emission of the polymeric complex is considerably red-shifted relative to **2**−**4** with a broad emission band appearing at 533 nm. The emission intensity of all compounds increases notably upon cooling of the solids to 77 K. However, the emission maxima only change slightly to 517, 509, and 514 nm for **2**−**4**, respectively.

DISCUSSION

Our earlier work with the dissymmetric MeimCH$_2$py ligand produced butterfly-shaped Cu_2X_2 clusters with very short Au···$Cu_{2(centroid)}$ distances of 2.541 to 2.586 Å,[27] and it is somewhat surprising that the symmetrically substituted ligand im$(CH_2py)_2$ did not afford similar motifs. The addition of excess CuX did not yield the butterfly-Cu_2X_2-containing species, and in fact only in the case of excess CuBr could a single product be cleanly isolated. Reducing the stoichiometry to two equivalents of CuX per $[Au(NHC)_2]^+$ moiety, however, readily yielded **2** and **3** in good yield and **4** in poor yield. The reason for this discrepancy is unknown but may reflect the inability of gold(I) to act as a metalloligand simultaneously to two other metal centers. The coordination motif of the NHC ligands in **2**−**4** is interesting. Coordination of a Cu(I) center to the two picolyl groups of the same ligand positions the carbene carbon in close contact with the copper center, producing a semibridging carbene. The Cu1−C1 separations of ∼2.05 Å are quite short, indicating strong interactions. The fact that these separations inversely track the Au1−C1 separations indicates that their electronic influence is real and not simply an artifact of constraint imposed by the chelating nature of the bispicolyl ligand. Further, a similar coordination motif was observed $[Au(im(CH_2py)_2)_2(Ag(CH_3CN))_2](BF_4)_3$,[16] where the two picolyl groups each chelate a silver center, however, in a more symmetrical fashion. It is interesting to note that in this complex the corresponding contacts between the chelated Ag(I) ions and the carbene carbon atoms are considerably longer at ∼2.7 Å, and the NHCs are not considered to be semibridging.

dx.doi.org/10.1021/ic201795b |*Inorg. Chem.* 2011, 50, 11228–11234

Furthermore, the observation of long Au−Ag separations (>3.2 Å) in $[Au(im(CH_2py)_2)_2(Ag(CH_3CN))_2](BF_4)_3$ further demonstrates that the short Au(I)−Cu(I) separations measured in **2**−**4**, and hence the Cu−$C_{carbene}$ separations, are not an artifact of ligand chelation.

Semibridging NHC carbon atoms are quite rare and only known of in a few homometallic systems. Han et al.[34] reported a Cu(I) dimer with a semibridging sulfur-containing NHC that has a short Cu−C separation of 1.978(9) Å and a semibridging Cu−C separation of 2.285(9) Å. Likewise Díez-González et al.[35] reported similar Cu−C separations of 1.973(8) and 2.165(8) in an NHC−CuBr cluster. With a related ligand set to the one reported here, Youngs and co-workers[36] characterized a semibridging NHC in a Ag_4−cyclophane complex with Ag−C separations of 2.149(6) and 2.516(6) Å. In 2005, we reported a triangular Ag_3−NHC complex that contained two fully bridging and one semibridging carbene with short/long Ag−C separations of 2.140(8) and 2.459(8) Å.[18] Fully bridging carbenes are more common and have been observed in a small number of homometallic Cu and Ag NHC complexes[21,37−41] and have been observed in gold−copper aryl complexes.[24,29] Youngs and co-workers were able to resolve the σ and π components of their bridging carbene by examining ^{13}C coupling to Ag in the ^{13}C NMR spectra, though it is unclear whether the NHC remains semibridging in solution. The work of Han et al.[34] would suggest otherwise. The lack of an NMR-active metal (I = 1/2) in the complexes reported here prevents a similar analysis, but the ^{13}C chemical shift of the carbene carbon atom is shifted presumably by the observed Cu−$C_{carbene}$ interaction. The ^{13}C CP-MAS NMR of **2** shows a single strong carbene resonance at 171.6 ppm, upfield from that of the starting material at 187.2 ppm (see the Supporting Information, Figure S15). The observed shielding effect upon coordination of CuCl is consistent with earlier results of silver complexes with bridging NHC ligands[40,41] whose ^{13}C resonances are found upfield of that in $[Ag(im(CH_2py)_2)_2]PF_6$ (see the Supporting Information).

The Au−Cu distances in **2**−**4** are slightly shorter than the 2.7915(7) Å separation measured in the related $[Au(im(CH_2py)_2)_2(Cu(MeOH))_2]^{3+}$ complex which contains the same bridging NHC ligand used here.[17] A large number of unsupported Au(I)−Cu(I) separations ranging from 2.9335(11) to 2.5741(6) Å have been observed in the ionic complexes $[(RCN)_nCu][Au(C_6F_5)_2]$[13,29] and $[(RCN)_n(C_4H_4N_2)Cu][Au(C_6X_5)_2]$.[24] Similar to the semibridging ligation described here, the copper atom in many of these complexes exhibits a π interaction with the *ipso* carbon of the perfluorophenyl group. In 2010, Gimeno and co-workers[32] reported a phosphinopyridyl-bridged Au(I)−Cu(I) complex with fairly long intermetallic separations of ∼3.0 Å. Using the same ligand system, Wang and co-workers[42] discovered much shorter separations ranging from 2.75 to 2.90 Å in a Au_6Cu_2 cluster. Eisenberg and co-workers[43] reported a very short Cu−Au interaction of 2.6339(7) Å in the mixed-ligand complex $[\{AuCu(\mu\text{-Spy})(\mu\text{-PPh}_2\text{py})\}_2](PF_6)_2$ that contains a three-coordinate Cu(I) center. Longer separations of ∼2.9 to 3.0 Å were found by Gimeno and co-workers[44] in the chalcogenide-capped $[EAu_3Cu(PPh_2py)_3]^{2+}$ (E = O, S, Se) clusters. The Cu−N and Cu−Br bond lengths in **5** are comparable to other pyridyl-bridged halide clusters $[Cu_2(\mu\text{-Br})_2L_4]$ (L = pyridine donor);[45−48] however, the Cu···Cu separation of 2.9248(14) Å in **5** is considerably longer than the 2.6 Å separation measured in the $[AuCu_2Br_2(CH_3imCH_2quin)_2]^+$ and $[AuCu_2Br_2(CH_3imCH_2py)_2]^+$ complexes.[45]

The luminescence behavior of **2**−**4** does not follow a trend due to halide discounting a XLCT assignment;[49] however, a large number of other possibilities exist.[50] In a recent report of complexes exhibiting short and unsupported Au···Cu contacts where Cu(I) is coordinated to a nitrile and pyrimidine,[24] a metal-to-ligand charge transfer was determined to be the likely origin of the luminescence process, and in **2**−**4**, a similar charge transfer from the metal atoms to the pyridine groups may also be responsible for the luminescence. While the emission maxima in **2**−**4** trend with the Au···Cu distances in the solid state, other parameters may be responsible for the small differences in λ_{max}. Likewise, the lack of a Au−Cu interaction in **5** and its relatively similar, yet slightly red-shifted, emission further discounts the role of Au−Cu interactions as the origin of the emissive state in **2**−**4**.

CONCLUSIONS

Several new 2:1 copper(I) halide adducts with the tetradentate $[Au(im(CH_2py)_2)_2]PF_6$ were characterized, and their similar luminescence behavior was interpreted to be independent of the halide ligand at the copper atoms. Molecular structures revealed short Au···Cu interactions and semibridging NHC ligands which can be observed in the solid-state CP-MAS ^{13}C NMR chemical shift, affording a convenient tool for the determination of the bonding situation with NHC ligands where X-ray molecular structures are unavailable.

EXPERIMENTAL SECTION

Commercial CuCl was purified by a literature method.[51] CuBr was precipitated from an aqueous $CuBr_2$ solution with SO_2. CuI (Acros) was used as received. Compound **1** was prepared according to the literature procedure.[16]

Solid-state MAS NMR spectra were recorded on a Tecmag Discovery 400 instrument, ^{13}C CP-MAS spectra were referenced to adamantane (CH signal at 37.85 ppm), ^{19}F MAS spectra to $NaBF_4$, and ^{31}P MAS spectra to KH_2PO_4. Solution NMR spectra were recorded on a Varian NMR System 500 instrument and referenced to residual solvent signals. Mass spectra were recorded on an Agilent Technologies 6230 TOF-MS instrument under electrospray ionization; masses are given with ^{35}Cl, ^{63}Cu, and ^{79}Br isotopes.

Single-crystal X-ray diffraction was performed on a Bruker SMART Apex CCD instrument at 100 K using graphite-monochromated Mo Kα radiation; crystals were immersed in Paratone oil and mounted on glass fibers. Data were corrected for Lorentz and polarization effects using the SAINT program and corrected for absorption using SADABS.[52,53] The structures were solved by direct methods or Patterson syntheses and refined using SHELXS and SHELXL[54] in the Olex2 software environment.[55] Figures were created with 50% probability ellipsoids.

Bis{μ_2-η^3-1,3-bis[(2-pyridyl-1κN)methyl]-2*H*-imidazol-2-ylidene-1,2κ^2C}di(chloro-1κ)dicopper(I)gold(I), 2(*Au*−*Cu*) Hexafluorophosphate, 2. A Schlenk flask was charged with 50 mL of acetonitrile, and the solvent was degassed by two freeze−thaw cycles. Solid **1** (199.8 mg, 237 μmol) and CuCl (47.0 mg, 0.48 mmol, 2 equiv) were added, and the suspension was stirred overnight. The resulting homogeneous solution was concentrated *in vacuo* until solids started to precipitate and then was layered with an equal volume of deoxygenized diethyl ether. Storage at −5 °C for a week yielded colorless crystals of **2** suitable for X-ray diffraction. Yield: 157 mg (64%). The product is very sensitive to oxygen in solution. ^1H NMR (499.8 MHz, CD_3CN, 25 °C): δ 8.47 (d, 4H, ^3J = 4.7 Hz, H-6 py), 7.68 (m, 4H, H-4 py), 7.30 (s, 4H, H-4/5 im), 7.25 (m, 4H, H-5 py), 7.18 (d, 4H, ^3J = 7.9 Hz, H-3 py), 5.42 (s, 8H, CH_2). $^{13}C\{^1H\}$ NMR (125.7 MHz, CD_3CN, 25 °C): δ 186.1

(CAu), 156.6 (C-2 py), 150.8 (C-6 py), 138.5 (C-4 py), 124.5, 124.0, 123.2, 57.0 (CH_2). Solid-state ^{13}C CP-MAS NMR (100.5 MHz, 20 °C): δ 171.6 (CAu), 153.4, 152.1, 151.0, 149.2, 138.9, 136.5, 125.0, 121.2, 123.1, 53.8 (CH_2). MS (ESI+) *m*/*z*: 893.0041 ($C_{30}H_{28}AuCl_2Cu_2N_8^+$ requires 893.0066).

Bis{μ_2-η^3-1,3-bis[(2-pyridyl-1κN)methyl]-2*H*-imidazol-2-ylidene-1,2$\kappa^2 C$}di(bromo-1κ)dicopper(I)gold(I), 2(*Au*−*Cu*) Hexafluorophosphate, 3. The compound was prepared in the same way as **2** using **1** (163.1 mg, 194 μmol) and CuBr (55.9 mg, 390 μmol). The suspension was heated to 40 °C, effecting dissolution of all solids. Yield: 162 mg (74%) of colorless needles suitable for X-ray crystallography. ^1H NMR (499.8 MHz, CD_3CN, 25 °C): 8.47 (m, 4H, H-6 py), 7.68 (td, 4H, ^3J = 7.8 Hz, ^4J = 1.8 Hz, H-4 py), 7.30 (s, 4H, H-4/5 im), 7.26 (m, 4H, H-5 py), 7.18 (m, 4H, H-3 py), 5.43 (s, 8H, CH_2). $^{13}C\{^1H\}$ (125.7 MHz, CD_3CN, 25 °C): 185.7 (CAu), 156.5 (C-2 py), 150.8 (C-6 py), 138.4 (C-4 py), 124.5, 123.9, 123.2, 56.8 (CH_2). Solid-state ^{13}C CP-MAS NMR (100.5 MHz, 20 °C): 171.2 (CAu), 156, 151, 138, 124−122, 56 (CH_2). MS (ESI+) *m*/*z*: 980.9033 ($C_{30}H_{28}AuBr_2Cu_2N_8^+$ requires 980.9056).

Bis{μ_2-η^3-1,3-bis[(2-pyridyl-1κN)methyl]-2*H*-imidazol-2-ylidene-1,2$\kappa^2 C$}di(iodo-1κ)dicopper(I)gold(I), 2(*Au*−*Cu*) Hexafluorophosphate, 4. The compound was prepared in the same way as **2** using **1** (160.6 mg, 191 μmol) and CuI (72.8 mg, 382 μmol). At first, a hazy suspension was obtained, giving a clear solution after 10 min. After 1 h, a precipitate formed that was dissolved by heating to 75 °C. Slow cooling resulted in little precipitate that was discarded and the mother liquor layered with an equal amount of deoxygenized diethyl ether. Yield: 10.4 mg (0.7%) of colorless crystals. The compound is not soluble enough to give a ^{13}C NMR spectrum. ^1H NMR (499.8 MHz, CD_3CN, 25 °C): 8.46 (m, 4H, H-6 py), 7.68 (m, 4H, H-4 py), 7.29 (s, 4H, H-4/5 im), 7.25 (m, 4H, H-5 py), 7.17 (m, 4H, H-3 py), 5.42 (s, 8H, CH_2). MS (ESI^+) *m*/*z*: 1076.8839 ($C_{30}H_{28}AuCu_2I_2N_8^+$ requires 1076.8779).

Catena-poly-bis{μ_3-η^3-1,3-bis[(2-pyridyl-1κN)methyl]-2*H*-imidazol-2-ylidene-1κC}di(μ_2-bromo-1κ^2)dicopper(I)gold(I), (*Cu*−*Cu*) Bromide, 5. $[Au(im(CH_2py)_2)_2]PF_6$ (150.3 mg, 178 μmol) was dissolved in 50 mL of deoxygenized acetonitrile, and CuBr (102 mg, 714 μmol) was added. The solution was heated until all precipitates dissolved and was slowly cooled to room temperature overnight. Crystals of $\mathbf{5}\cdot 3CH_3CN$ formed that were suitable for X-ray crystallography. The crystals were isolated and dried *in vacuo*, yield: 77.0 mg (40.6%). ^1H NMR [499.8 MHz, $(CD_3)_2SO$, 25 °C]: δ 8.49 (m, 4H, H-6 py), 7.76 (td, ^3J = 7.7 Hz, ^4J = 1.6 Hz, 4H, H-4 py), 7.61 (s, 4H, H-4/5 im), 7.33 (m, 4H, H-5 py), 7.26 (m, 4H, H-3 py), 5.50 (s, 8H, CH_2), 2.07 (s, 8H, CH_3CN). $^{13}C\{^1H\}$ [125.7 MHz, $(CD_3)_2SO$, 25 °C]: δ 183.1, 155.2, 149.4, 137.4, 123.3, 123.1, 122.2, 118.0, 55.0, 1.1. Solid-state ^{13}C CP-MAS NMR (100.5 MHz, 20 °C): 185.5 (CAu), 156.6, 150.6, 140.5, 137.1, 126.0, 124.6, 123.7, 122.6, 121.1, 56 (br), 0.2 (CH_3CN). MS (ESI+) *m*/*z*: 454.8979 ($C_{15}H_{14}BrCu_2N_4^+$ requires 454.898830), 588.9348 ($C_{15}H_{14}AuBrCuN_4^+$ requires 588.935801), 730.7807 ($C_{15}H_{14}AuBr_2Cu_2N_4^+$ requires 730.787358), 839.0532 ($C_{30}H_{28}AuBrCuN_8^+$ requires 839.057648), 980.9016 ($C_{30}H_{28}AuBr_2Cu_2N_8^+$ requires 980.905582).

■ ASSOCIATED CONTENT

Supporting Information. X-ray crystallographic data for the complexes in CIF format, solid state MAS NMR, and optical and mass spectra. This material is available free of charge via the Internet at http://pubs.acs.org.

■ AUTHOR INFORMATION

Corresponding Author
*E-mail: vjc@unr.edu.

■ ACKNOWLEDGMENT

This material is based upon work supported by the National Science Foundation under Grant No. CHE-0549902.

■ REFERENCES

(1) Herrmann, W. A. *Angew. Chem., Int. Ed.* **2002**, *41*, 1290–1309.
(2) Fortman, G. C.; Nolan, S. P. *Chem. Soc. Rev.* **2011**, *40*, 5151−5169.
(3) Lin, J. C. Y.; Huang, R. T. W.; Lee, C. S.; Bhattacharyya, A.; Hwang, W. S.; Lin, I. J. B. *Chem. Rev.* **2009**, *109*, 3561–3598.
(4) Schmidbaur, H.; Schier, A. *Z. Naturforsch., B: Chem. Sci.* **2011**, *66*, 329–350.
(5) Ackermann, L. *Angew. Chem., Int. Ed.* **2011**, *50*, 3842–3844.
(6) Nolan, S. P. *Acc. Chem. Res.* **2011**, *44*, 91–100.
(7) Díez-Gonzalez, S.; Stevens, E. D.; Scott, N. M.; Petersen, J. L.; Nolan, S. P. *Chem.—Eur. J.* **2008**, *14*, 158–168.
(8) Ellul, C. E.; Reed, G.; Mahon, M. F.; Pascu, S. I.; Whittlesey, M. K. *Organometallics* **2010**, *29*, 4097–4104.
(9) Garrison, J. C.; Youngs, W. J. *Chem. Rev.* **2005**, *105*, 3978–4008.
(10) Lin, I. J. B.; Vasam, C. S. *Comment. Inorg. Chem.* **2004**, *25*, 75–129.
(11) Rodríguez-Castillo, M.; Monge, M.; López-de-Luzuriaga, J. M.; Olmos, M. E.; Laguna, A.; Mendizabal, F. *Comput. Theor. Chem.* **2011**, *965*, 163–167.
(12) Sculfort, S.; Braunstein, P. *Chem. Soc. Rev.* **2011**, *40*, 2741–2760.
(13) Fernández, E. J.; Laguna, A.; López-de-Luzuriaga, J. M.; Monge, M.; Montiel, M.; Olmos, M. E.; Rodríguez-Castillo, M. *Dalton Trans.* **2009**, 7509–7518.
(14) Fernández, E. J.; Laguna, A.; López-de-Luzuriaga, J. M. *Dalton Trans.* **2007**, 1969–1981.
(15) Muñiz, J.; Wang, C.; Pyykkö, P. *Chem.—Eur. J.* **2011**, *17*, 368–377.
(16) Catalano, V. J.; Malwitz, M. A.; Etogo, A. O. *Inorg. Chem.* **2004**, *43*, 5714–5724.
(17) Strasser, C. E.; Catalano, V. J. *J. Am. Chem. Soc.* **2010**, *132*, 10009–10011.
(18) Catalano, V. J.; Moore, A. L. *Inorg. Chem.* **2005**, *44*, 6558–6566.
(19) Tulloch, A. A. D.; Danopoulos, A. A.; Kleinhenz, S.; Light, M. E.; Hursthouse, M. B.; Eastham, G. *Organometallics* **2001**, *20*, 2027–2031.
(20) Zhou, Y.; Chen, W. *Organometallics* **2007**, *26*, 2742–2746.
(21) Liu, B.; Chen, W.; Jin, S. *Organometallics* **2007**, *26*, 3660–3667.
(22) Ghosh, A. K.; Catalano, V. J. *Eur. J. Inorg. Chem.* **2009**, 1832–1843.
(23) Catalano, V. J.; Etogo, A. O. *J. Organomet. Chem.* **2005**, *690*, 6041–6050.
(24) López-de-Luzuriaga, J. M.; Monge, M.; Olmos, M. E.; Pascual, D.; Rodríguez-Castillo, M. *Inorg. Chem.* **2011**, *50*, 6910–6921.
(25) Laguna, A.; Lasanta, T.; López-de-Luzuriaga, J. M.; Monge, M.; Naumov, P.; Olmos, M. E. *J. Am. Chem. Soc.* **2010**, *132*, 456–457.
(26) Luquin, A.; Elosúa, C.; Vergara, E.; Estella, J.; Cerrada, E.; Bariáin, C.; Matías, I. R.; Garrido, J.; Laguna, M. *Gold Bull.* **2007**, *40*, 225–233.
(27) Catalano, V. J.; Moore, A. L.; Shearer, J.; Kim, J. *Inorg. Chem.* **2009**, *48*, 11362–11375.
(28) Rios, D.; Olmstead, M. M.; Balch, A. L. *Inorg. Chem.* **2009**, *48*, 5279–5287.
(29) Fernández, E. J.; Laguna, A.; López-de-Luzuriaga, J. M.; Monge, M.; Montiel, M.; Olmos, M. E.; Rodríguez-Castillo, M. *Organometallics* **2006**, *25*, 3639–3646.
(30) Fernández, E. J.; Laguna, A.; López-de-Luzuriaga, J. M.; Montiel, M.; Olmos, M. E.; Pérez, J. *Organometallics* **2005**, *24*, 1631–1637.
(31) Fernández, E. J.; Laguna, A.; López-de-Luzuriaga, J. M.; Monge, M.; Nema, M.; Olmos, M. E.; Pérez, J.; Silvestru, C. *Chem. Commun.* **2007**, 571–573.
(32) Calhorda, M. J.; Ceamanos, C.; Crespo, O.; Gimeno, M. C.; Laguna, A.; Larraz, C.; Vaz, P. D.; Villacampa, M. D. *Inorg. Chem.* **2010**, *49*, 8255–8269.

(33) Sculfort, S.; Welter, R.; Braunstein, P. *Inorg. Chem.* **2010**, *49*, 2372–2382 and references cited therein.
(34) Han, X.; Koh, L. L.; Liu, Z.-P.; Weng, Z.; Hor, T. S. A. *Organometallics* **2010**, *29*, 2403–2405.
(35) Díez-González, S.; Escudero-Adán, E. C.; Benet-Buchholz, J.; Stevens, E. D.; Slawin, A. M. Z.; Nolan, S. P. *Dalton Trans.* **2010**, *39*, 7595–7606.
(36) Garrison, J. C.; Simons, R. S.; Kofron, W. G.; Tessier, C. A.; Youngs, W. J. *Chem. Commun.* **2001**, 1780–1781.
(37) Liu, B.; Zhang, Y.; Xu, D.; Chen, W. *Chem. Commun.* **2011**, *47*, 2883–2885.
(38) Mrutu, A.; Dickie, D. A.; Goldberg, K. I.; Kemp, R. A. *Inorg. Chem.* **2011**, *50*, 2729–2731.
(39) Gischig, S.; Togni, A. *Organometallics* **2005**, *24*, 203–205.
(40) Catalano, V. J.; Malwitz, M. A. *Inorg. Chem.* **2004**, *42*, 5483–5485.
(41) Catalano, V. J.; Munro, L. B.; Strasser, C. E.; Samin, A. F. *Inorg. Chem.* **2011**, *50*, 8465–8476.
(42) Jia, J.-H.; Liang, J.-X; Lei, Z.; Cao, Z.-X.; Wang, Q.-M. *Chem. Commun.* **2011**, *47*, 4739–4741.
(43) Hao, L.; Mansour, M. A.; Lachicotte, R. J.; Gysling, H. J.; Eisenberg, R. *Inorg. Chem.* **2000**, *39*, 5520–5529.
(44) Crespo, O.; Gimeno, M.; Laguna, A.; Larraz, C.; Villacampa, M. *Chem.—Eur. J.* **2007**, *13*, 235–246.
(45) Skelton, B. W.; Waters, A. F.; White, A. L. *Aust. J. Chem.* **1991**, *44*, 1207–1215.
(46) Healy, P. C.; Pakawatchai, C.; White, A. L. *J. Chem. Soc., Dalton Trans.* **1985**, 2531–2539.
(47) Dyason, J. C.; Engelhardt, L. M.; Healy, P. C.; Pakawatchai, C.; White, A. L. *Inorg. Chem.* **1985**, *24*, 1950–1957.
(48) Ghosh, M.; Biswas, P.; Flörke, U.; Nag, K. *Inorg. Chem.* **2008**, *47*, 281–296.
(49) Araki, H.; Tsuge, K.; Sasaki, Y.; Ishizaka, S.; Kitamura, N. *Inorg. Chem.* **2005**, *44*, 9667–9675.
(50) Ford, P. C.; Cariati, E.; Bourassa, J. *Chem. Rev.* **1999**, *99*, 3625–3647.
(51) Vaidya, B. K. *Nature* **1929**, *123*, 414.
(52) *SAINT*, version 7.68A; Bruker AXS: Madison, WI, 2009.
(53) *SADABS*, version 2008/1; Bruker AXS: Madison, WI, 2009.
(54) Sheldrick, G. M. *Acta Crystallogr., Sect. A: Found. Crystallogr.* **2008**, *64*, 112–122.
(55) Dolomanov, O. V.; Bourhis, L. J.; Gildea, R. J.; Howard, J. A. K.; Puschmann, H. *J. Appl. Crystallogr.* **2009**, *42*, 339–341.